XXX Nonlinear Session

Numerical Study of the Free Surface Magnetohydrodynamic Wave Turbulence

Evgeny Kochurin[1,2], Guillaume Ricard[3], Nikolay Zubarev[2,4], Eric Falcon[3]

[1]Skolkovo Institute of Science and Technology, Moscow, Russia
[2]Institute of Electrophysics, Ural Division of RAS, Ekaterinburg, Russia
[3]Université de Paris, Univ. Paris Diderot, Paris, France
[4]P.N. Lebedev Physical Institute, Russian Academy of Sciences, Moscow, Russia
E-mail:kochurin@iep.uran.ru

December, 2021

Wave turbulence theory (Kolmogorov-Zakharov's spectrum)

Wave turbulence occurs when nonlinear waves interact with each other. This phenomenon is ubiquitous: oceanographic waves, plasma waves in the solar wind, nonlinear optical waves, elastic waves, or gravitational waves. A weakly nonlinear theory (or weak turbulence theory) predicts analytically the wave spectra in various domains involving nonlinear waves. Such Kolmogorov-Zakharov's (KZ) spectra can be also obtained by dimensional analysis, [Nazarenko et al. (2003)].

The Zakharov-Filonenko spectrum (1967) for isotropic capillary wave turbulence is the example of KZ-spectrum:

$$S(\mathbf{k}) = < |\eta_{\mathbf{k}}|^2 > = C(\sigma/\rho)^{-3/4} P^{1/2} k^{-(19/4)},$$

where C is a constant, σ is the surface tension coefficient, ρ is the mass density of a liquid, P is the energy dissipation rate.

Capillary turbulence of a free surface / A picture from the internet

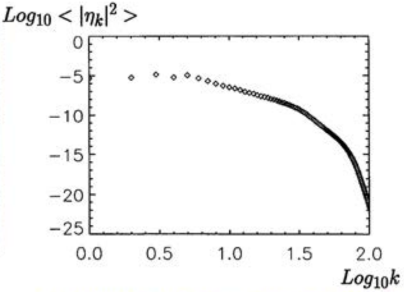

A. N. Pushkarev, V. E. Zakharov / Phys. Rev. Lett. (1996)

Magnetic (electric) free surface wave turbulence

A new type of magnetohydrodynamic turbulence developing in an external magnetic (electric) field at the free surface of a liquid was discovered in the works [Boyer,Falcon, (2008), Dorbolo, Falcon (2011)]. There was no theoretical explanation for this phenomenon. In our works [Kochurin, E.A. JETP Lett. (2019), Kochurin, E.A. J. Magn. Magn. Mater. (2020)], for the first time, the new type of magnetohydrodynamic turbulence was numerically simulated in the case of plane-symmetric geometry. A new type of turbulence spectrum is observed both numerically and experimentally.

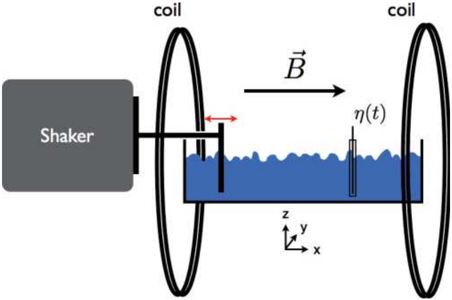

[1] F. Boyer, E. Falcon. Phys. Rev. Lett. (2008).
[2] S. Dorbolo, E. Falcon. Phys. Rev. 2011

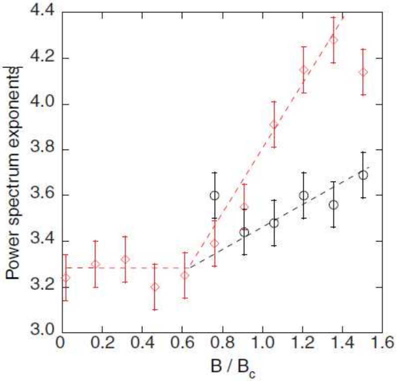

Dimensional derivation of Kolmogorov-Zakharov's spectra

Consider a wave system with the linear dispersion law

$$\omega(\mathbf{k}) = \lambda k^{\alpha}, \tag{1}$$

where ω is the frequency, $\mathbf{k}$ is the wave vector, and $k = |\mathbf{k}|$ is its absolute value. The important feature of the wave system is the number of waves N involved in resonant interaction. The number N is defined as a minimal integer for which the N-wave resonant conditions are satisfied:

$$\omega(\mathbf{k}_1) \pm \omega(\mathbf{k}_2) \ldots \pm \omega(\mathbf{k}_N) = 0, \;\; \mathbf{k}_1 \pm \mathbf{k}_2 \ldots \pm \mathbf{k}_N = 0. \tag{2}$$

Write now the formula for the turbulence spectrum in terms of the energy density for a N-wave system:

$$E_k = CP^{1/(N-1)} \lambda^X k^Y, \tag{3}$$

where E_k is the spectral energy density in absolute k, C is the Kolmogorov-Zakharov's constant. The indexes X and Y are defined as,

$$X = \frac{2N-5}{N-1}, \quad Y = (2\alpha + d - 6) + \frac{5 - 3\alpha - d}{N-1},$$

where d is the dimension in the physical space of the energy density E_k (E_k has dimension $L^{6-d}T^{-2}$, $[S(k)] = L^{5-d}$, and $[P] = L^{5-d}T^{-3}$). Let us introduce the dimension of Fourier space D. In the case of anisotropic geometry, d and D are not equal to each other. The spectral energy density is related with the wave action $n(\mathbf{k})$ as follows, $\int E_k dk = \int \omega_{\mathbf{k}} n(\mathbf{k}) d\mathbf{k} = \Omega_D \int \omega_{\mathbf{k}} n(\mathbf{k}) k^{D-1} dk$, where Ω_D is the solid angle in Fourier space.

Kolmogorov-Zakharov's spectra for capillary wave turbulence

In the case of isotropic two-dimensional capillary wave turbulence $d = D = 2$, $N = 3$, the relation (3) yield the classic example of Zakharov-Filonenko spectrum (1968):

$$n(\mathbf{k}) = C_{2D}^{3w} P^{1/2} (\sigma/\rho)^{-1/4} k^{-17/4}.$$

$$E_k = 2\pi C_{2D}^{3w} P^{1/2} (\sigma/\rho)^{1/4} k^{-7/4}. \tag{4}$$

For the capillary waves, the energy density E_k is related with the surface elevation spectrum as follows $E_k = (\sigma/\rho)\Omega_D k^2 |\eta_{\mathbf{k}}|^2 k^{D-1}$, where $\eta_{\mathbf{k}}$ is the Fourier image of the function $\eta(x, y)$ determining the shape of a free surface. Thus, from the expression (4) one can obtain the spectra $S(\mathbf{k}) = |\eta_{\mathbf{k}}|^2$ and $S(\omega) = |\eta_\omega|^2$ for the surface elevation in k and ω domains, respectively:

$$S(\mathbf{k}) = C_{2D}^{3w} P^{1/2} (\sigma/\rho)^{-3/4} k^{-19/4}, \tag{5}$$

$$S(\omega) = 4\pi/3 C_{2D}^{3w} P^{1/2} (\sigma/\rho)^{1/6} \omega^{-17/6}. \tag{6}$$

The spectrum (6) is obtained from the relation $S(\mathbf{k})d\mathbf{k} = S(\omega)d\omega$, which has a sense of the conservation law of energy in k and ω coordinates. The spectra (5) and (6) are well known and confirmed both experimentally and numerically [N Pushkarev and V E Zakharov. Phys. Rev. Lett (1996), M Yu Brazhnikov, G V Kolmakov, A A Levchenko, L P Mezhov-Deglin. JETP Lett., (2001), E Falcon, C Laroche, S Fauve. Phys. Rev. Lett., (2007)].

What happens when an external magnetic field is applied?

Dimensional derivation of the Phillips spectrum

Note that for gravity waves of large amplitude, the Phillips spectrum (1958) can be realized

$$[S(\mathbf{k})] = L^4, \qquad \rightarrow \qquad S(\mathbf{k}) = f(\theta)k^{-4}, \tag{7}$$

$$[S(\omega)] = L^2 T, \qquad \rightarrow \qquad S(\omega) = \alpha g^2 \omega^{-5}, \tag{8}$$

with α is the non-dimensional Phillips constant. The Phillips spectrum (15) is sufficiently different from the weakly turbulent KZ spectra: it does not explicitly depend on the energy dissipation flux P. The independence of the Phillips spectrum from the input energy is caused by the wave breaking processes in nonlinear wave systems [Kuznetsov, JETP Lett. (2004)]. The Phillips spectrum can be realized for nondispersive quasi-shock wave turbulence of gravity waves in shallow waters.

The derivation of the Phillips spectrum can be easily generalized for capillary waves with the dispersion law, $\omega = (\sigma/\rho)^{1/2}k^{3/2}$.

$$[S(\mathbf{k})] = L^4, \qquad \rightarrow \qquad S(\mathbf{k}) = g(\theta)k^{-4}, \tag{9}$$

$$[S(\omega)] = L^2 T, \qquad \rightarrow \qquad S(\omega) = \alpha_c \frac{2}{3}\left(\frac{\sigma}{\rho}\right)^{2/3}\omega^{-7/3}. \tag{10}$$

with α_c is the non-dimensional capillary Phillips constant. The capillary Phillips spectrum is predicted in the work [Newell, Zakharov, Phys. Lett. A (2008)]

Thus, there are two possible types of spectra for the wave turbulence on water surface: weakly nonlinear KZ spectra, and strongly nonlinear Phillips spectrum (9)-(10) .

What spectrum do we expect to observe in simulation of the free surface MHD wave turbulence?

he dispersion relation for linear waves at the boundary of a ferrofluid subjected to an external horizontal magnetic field B has the form [Melcher (1961)]:

$$\omega^2(\mathbf{k}) = gk + \frac{\gamma(\mu)}{\rho} B^2 k_x^2 + \frac{\sigma}{\rho} k^3, \tag{11}$$

where ω is the frequency, g is the gravitational acceleration, $\gamma(\mu) = (\mu - 1)^2/(\mu_0[\mu + 1])$ is the auxiliary coefficient, μ_0 and μ are the magnetic permeabilities of vacuum and liquid, respectively. For high magnetic fields, surface waves propagates along the x-axis without dispersion (like acoustic waves) with Alfèn speed, $V_A^2 = \gamma B^2/\rho$.

Assuming that effects of capillarity and gravity are negligible (wave propagation is non-dispersive), and the isotropic character of fluid motion, one can obtain the MHD turbulence spectra:

$$S(\mathbf{k}) = C_B^{\mathrm{KZ}} P^{1/2} V_A^{-3/2} k^{-4}, \tag{12}$$

$$S(\omega) = 2\pi C_B^{\mathrm{KZ}} P^{1/2} V_A^{1/2} \omega^{-3}, \tag{13}$$

where C_B^{KZ} is the Kolmogorov-Zakharov constant for the free surface MHD wave turbulence.

Surprisingly, that for the pure non-dispersive case in 2D geometry, the KZ-spectrum coincides with the Phillips spectrum

$$[S(\mathbf{k})] = L^4, \quad \rightarrow \quad S(\mathbf{k}) = \alpha_B k^{-4}, \tag{14}$$

$$[S(\omega)] = L^2 T, \quad \rightarrow \quad S(\omega) = \alpha_B V_A^2 \omega^{-3}. \tag{15}$$

if $\alpha_B = (P/V_A^3)^{1/2}$. The energy dissipation flux P has the same dimension as V_A^3.

Model equations

The computational model used in the work is based on the quadratically nonlinear equation system initialy formulated in the framework of Hamiltonian formalism for the description of electrohydrodynamic motion of dielectric liquids in [Zubarev (2004), Zubarev (2009), Zubarev and Kochurin (2013)]. Melcher has shown that ferrofluid MHD motion is mathematically completely equivalent to the dynamics of non-conducting liquids subjected to an external electric field, i.e., the model can be directly used for studying the current problem.

The Hamiltonian of the system under study in dimensionless units ($\rho = 1$, $\sigma = 1$) reads

$$\mathcal{H} = \frac{1}{2}\iint \Big[(\nabla_\perp \eta)^2 + \psi \hat{k}\psi - \eta\left((\hat{k}\psi)^2 - (\nabla_\perp \psi)^2 \right) + V_A^2 \Big(\eta_x \hat{k}^{-1}\eta_x + A_\mu \Big[\eta\eta_x^2 - \eta_x \hat{k}^{-1}\eta\hat{k}\eta_x + \eta_x \hat{k}^{-1}(\nabla_\perp \eta \cdot \nabla_\perp \hat{k}^{-1}\eta_x) \Big] \Big) \Big] \, dxdy, \qquad (16)$$

where $\nabla_\perp = \{\partial_x, \partial_y\}$ is the nabla operator, $\hat{k}$ is the integral operator having the form: $\hat{k}f_k = kf_k$, in the Fourier representation, $\hat{k}^{-1}$ is the inverse $\hat{k}$-operator, and $A_\mu = (\mu - 1)/(\mu + 1)$ is the magnetic Atwood number.

The equations of the boundary motion are obtained by taking the variational derivatives:

$$\frac{\partial \eta}{\partial t} = \frac{\delta H}{\delta \psi}, \qquad \frac{\partial \psi}{\partial t} = -\frac{\delta H}{\delta \eta}. \qquad (17)$$

The equations (17) of the boundary motion are applicable for any symmetry of the surface perturbations. In the quasi-1D geometry they can be simplified.

Finally, taking the variational derivatives from (16) and adding to the equations (17) terms responsible for the effects of pumping and dissipation of energy, one get the governing equation system:

$$\eta_t = \hat{k}\psi - \hat{k}(\eta\hat{k}\psi) - \nabla_\perp(\eta\nabla_\perp\psi) + \hat{D}_k\eta, \tag{18}$$

$$\psi_t = \nabla_\perp^2\eta + \frac{1}{2}\left[(\hat{k}\psi)^2 - (\nabla_\perp\psi)^2\right] + V_A^2\hat{k}^{-1}\eta_{xx}$$
$$-\frac{A_\mu V_A^2}{2}\left[2\hat{k}^{-1}\partial_x\left(\eta\hat{k}\eta_x - \nabla_\perp\eta\cdot\nabla_\perp\hat{k}^{-1}\eta_x\right) - \eta_x^2\right.$$
$$\left.-2\eta\eta_{xx} - (\nabla_\perp\hat{k}^{-1}\eta_x)^2\right] + \mathcal{F}(\mathbf{k},t) + \hat{D}_k\psi, \tag{19}$$

where $\hat{D}_k$ is the viscosity operator acting as, $\hat{D}_k f_k = -\nu(k-k_d)^2 f_k$, for $k \geq k_d$, and, $\hat{D}_k = 0$, for $k < k_d$, the coefficient ν determines the intensity of energy dissipation. The pumping term $\mathcal{F}(\mathbf{k},t)$ in (19) is defined in Fourier space as: $\mathcal{F}(\mathbf{k},t) = F(k)\exp[i(\omega(\mathbf{k}) + R)t]$, where $F(k) = F_0\exp[-(k-k_0)^4/k_f]$, with F_0 is the forcing amplitude reached at $k = k_0$, and R are the random numbers normally distributed at the interval $[0, 2\pi]$. The wave vectors are pumped at the range: $1 \leq k \leq k_f$. Thus, we use resonant forcing with isotropic set of wavenumbers but anisotropic distribution of frequencies.

We present four series of calculations with the different values of an external magnetic field: $V_A^2 = 0$, 25, 100, and 300, respectively. Figure 1 shows the temporal evolution of the total energy of the system defined from (16).

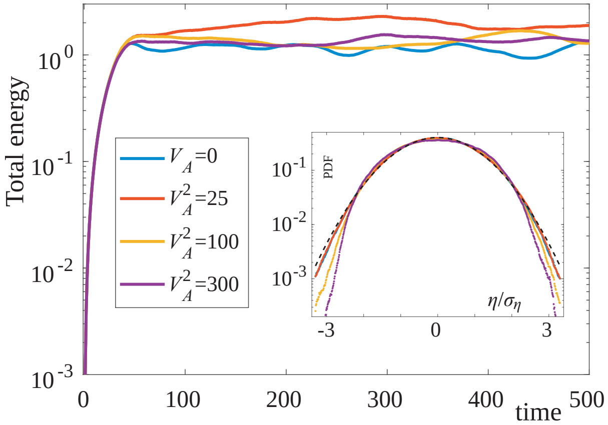

Figure 1: The free surface shape is shown at the time instant, $t = 250$, of a quasi-stationary state for the different values of a magnetic field: (a)-(d) correspond to $V_A^2 = 0$, 25, 100, and 300, respectively..

Figure 2 shows the free surface of a magnetic fluid at a given moment of a quasi-stationary state for the different magnetic fields. One can observe a transition from isotropic to highly anisotropic character of the fluid motion. In the case of maximal magnetic field, the surface relief becomes almost unidirectional; the surface waves propagate along the y-axis, i.e., in the direction perpendicular to the external magnetic field

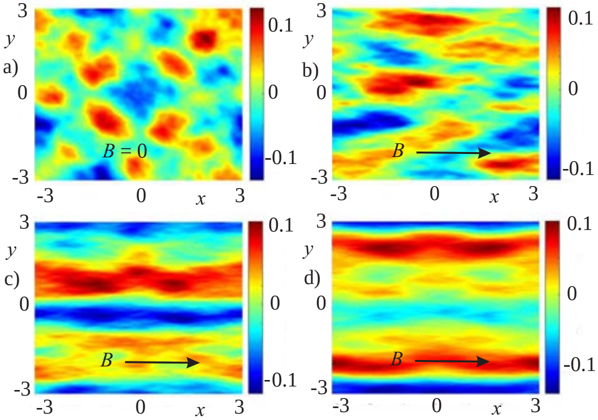

Figure 2: The free surface shape is shown at the time instant, $t = 250$, of a quasi-stationary state for the different values of a magnetic field: (a)-(d) correspond to $V_A^2 = 0$, 25, 100, and 300.

Figure 3 shows the free surface gradient at the same moments as in Fig. 2. Figure 3 clearly shows the tendency to formation of spatially narrow regions with sharp jumps in the surface gradient along y-axis. The time-averaged steepness was equal to 0.17, 0.18, 0.14, 0.17; and averaged absolute curvature (the second spatial derivative of η) was 1.43, 2.35, 2.94, and 3.95 for the corresponding values of V_A.

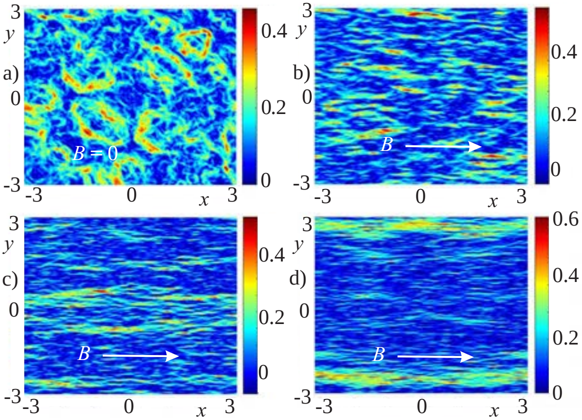

Figure 3: The free surface gradient is shown at the time instant, $t = 250$, of a quasi-stationary state for the different values of a magnetic field: (a)-(d) correspond to $V_A^2 = 0$, 25, 100, and 300, respectively.

Figure 4 shows the space-time surface spectrum for the waves traveling along the direction of an external field, i.e., with $k_y = 0$. Energy is found to be localized in the Fourier space around the linear dispersion relation (11).

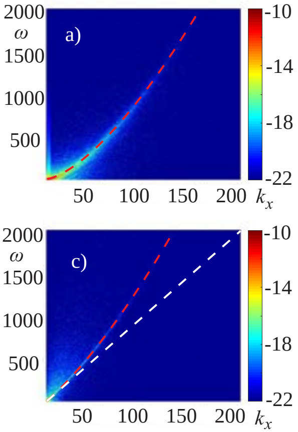

Figure 4: Space-time Fourier transform of the surface shape, $\log|\eta(\omega, k_x, 0)|$. The red dashed lines correspond to the dispersion relation (11) and white dashed lines to non-dispersive wave propagation, $\omega = V_A k_x$; (a)-(d) correspond to $V_A^2 = 0$, 25, 100, and 300, respectively

The space-time spectrum for the waves traveling along the y-axis is shown in Figure 5.In Figure 5, we see an evidence of a coherent structure in the form of a second additional branch of the dispersion curve. This branch is nothing else than bound waves propagating over the main carrier wave.

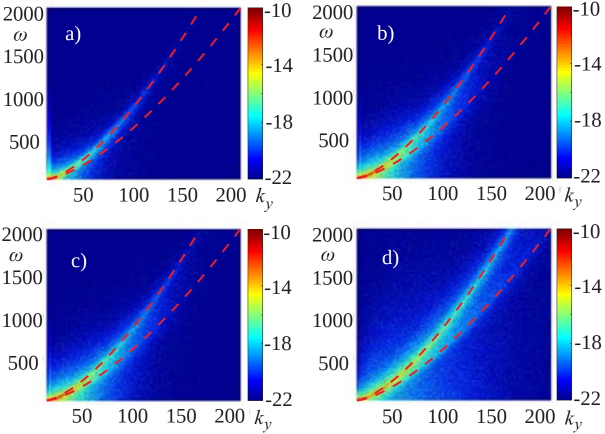

Figure 5: Space-time Fourier transform of the surface shape, log $|\eta(\omega, 0, k_y)|$. The red dashed lines correspond to the dispersion relations: $\omega = k_y^{3/2}$, and $\omega = k_y^{3/2}/2^{1/2}$; (a)-(d) correspond to $V_A^2 = 0$, 25, 100, and 300, respectively.

Figure 6 shows cross-sections of the surface elevation spectrum $S(\mathbf{k})$ along the x-axis (blue lines) and y-axis (green lines) for the different magnetic fields.

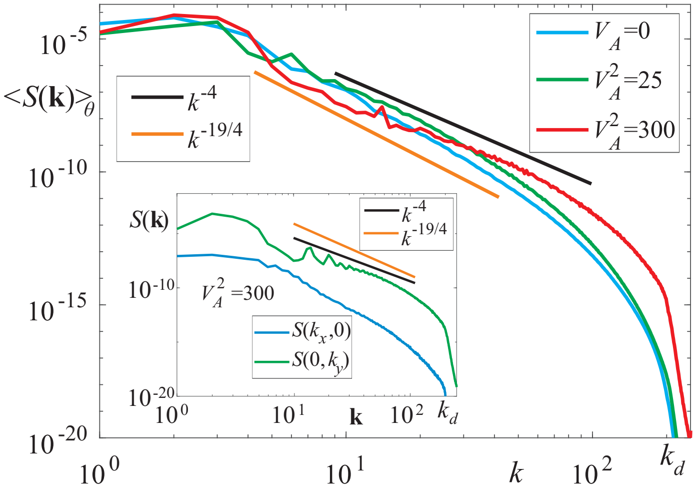

Figure 6: The cross-sections of the time-averaged spatial spectrum, $S(\mathbf{k})$, in $k_y = 0$ (blue lines) and in $k_x = 0$ (green lines). Insets: surface spectra averaged over phase angle and multiplied by k.

Figure 9 shows the frequency spectra $S(\omega)$ at zero and high magnetic fields. In the absence of a field, the simulation results again show good agreement with the KZ spectrum: $S(\omega) \sim \omega^{-17/6}$. However, at the strong field, the frequency spectrum does not coincide with the spectrum (13) for non-dispersive waves.

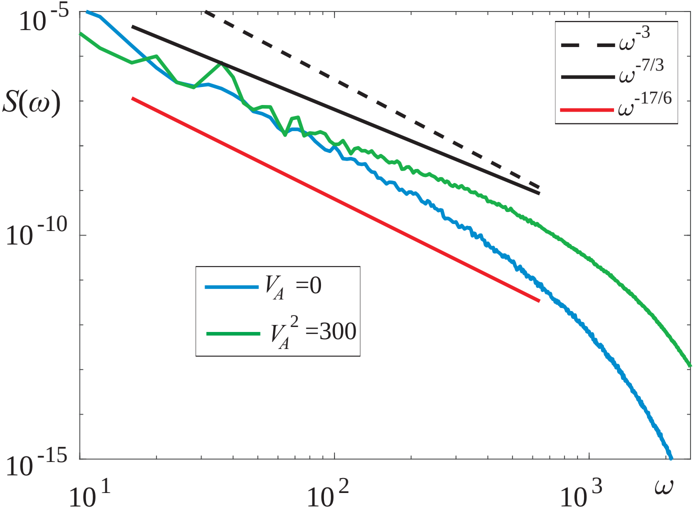

Figure 7: Frequency spectra of the surface elevation $S(\omega)$.

The three-wave resonance conditions

$$\mathbf{k} = \mathbf{k_1} + \mathbf{k_2}, \qquad \omega = \omega_1 + \omega_2.$$

To check the conditions for the realization of exact resonances, we used the third-order correlator (bicoherence)

$$B(k_1, k_2) = \frac{|\langle \eta^*_{k_1} \eta_{k_2} \eta_{k_1+k_2} \rangle|}{\sqrt{\langle |\eta_{k_1}|^2 \rangle \langle |\eta_{k_2} \eta_{k_1+k_2}|^2 \rangle}}, \qquad \mathbf{k_2} = \{0, 50\} \tag{20}$$

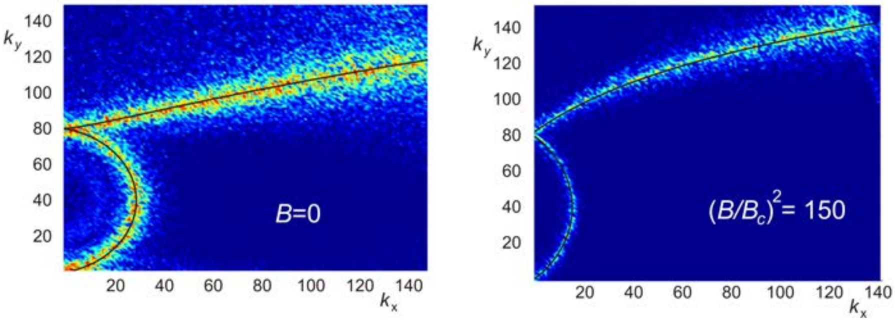

Figure 8: Bicoherence is shown for the zero field (left) and for VA2=150 (right).

The sectrumhe coefficients C_k and C_ω are measured in the quasi-stationary state

$$S(\mathbf{k}) = C_k k^{-4}, \qquad S(\omega) = C_\omega \omega^{-7/3}.$$

The simulation results show that

$$C_k \sim (P/V_A^3)^{1/2}, \qquad C_\omega \sim (P/V_A^3)^{1/2}$$

The quantity $\alpha_B = (P/V_A^3)^{1/2}$ is non-dimensional!

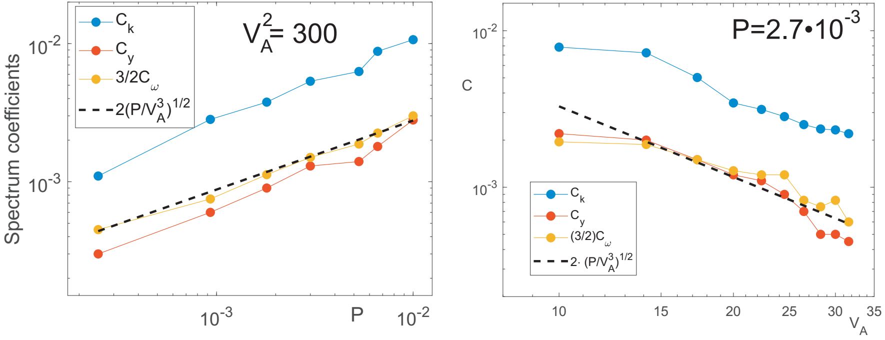

Figure 9: Spectra coefficients vs. energy flux P for $V_A = 0$ and $V_A^2 = 300$ (left), and vs. magnetic field (right).

Conclusion – Thus, with an increase in the external magnetic field, we observe a transition from the isotropic weak capillary turbulence to strongly anisotropic MHD turbulence, which is an ensemble of dispersive capillary shocks propagating in the direction perpendicular to a field. We believe that anisotropy arises as a result of the energy transfer from low-frequency magnetohydrodynamic waves to high-frequency capillary waves traveling perpendicular to the external magnetic field.

Acknowledgments – E.K. thanks partial support by Russian Science Foundation project No. No. 21-71-00006. E.F. thanks partial support of the French National Research Agency (ANR Dysturb, project No. ANR-17-CE30-0004), and of the Simons Foundation/MPS No. 651463-Wave Turbulence notably for the mission of E.K. in Paris, France.

E. Kochurin, G. Ricard, N. Zubarev, E. Falcon, Phys. Rev. Lett. (2021) in preparing

Thank you for your attention!